NASA/TM—2004–213282

Solid Rocket Booster Hydraulic Pump Port Cap Joint Load Testing

W.R. Gamwell and N.C. Murphy
Marshall Space Flight Center, Marshall Space Flight Center, Alabama

June 2004

The NASA STI Program Office…in Profile

Since its founding, NASA has been dedicated to the advancement of aeronautics and space science. The NASA Scientific and Technical Information (STI) Program Office plays a key part in helping NASA maintain this important role.

The NASA STI Program Office is operated by Langley Research Center, the lead center for NASA's scientific and technical information. The NASA STI Program Office provides access to the NASA STI Database, the largest collection of aeronautical and space science STI in the world. The Program Office is also NASA's institutional mechanism for disseminating the results of its research and development activities. These results are published by NASA in the NASA STI Report Series, which includes the following report types:

- TECHNICAL PUBLICATION. Reports of completed research or a major significant phase of research that present the results of NASA programs and include extensive data or theoretical analysis. Includes compilations of significant scientific and technical data and information deemed to be of continuing reference value. NASA's counterpart of peer-reviewed formal professional papers but has less stringent limitations on manuscript length and extent of graphic presentations.

- TECHNICAL MEMORANDUM. Scientific and technical findings that are preliminary or of specialized interest, e.g., quick release reports, working papers, and bibliographies that contain minimal annotation. Does not contain extensive analysis.

- CONTRACTOR REPORT. Scientific and technical findings by NASA-sponsored contractors and grantees.

- CONFERENCE PUBLICATION. Collected papers from scientific and technical conferences, symposia, seminars, or other meetings sponsored or cosponsored by NASA.

- SPECIAL PUBLICATION. Scientific, technical, or historical information from NASA programs, projects, and mission, often concerned with subjects having substantial public interest.

- TECHNICAL TRANSLATION. English-language translations of foreign scientific and technical material pertinent to NASA's mission.

Specialized services that complement the STI Program Office's diverse offerings include creating custom thesauri, building customized databases, organizing and publishing research results…even providing videos.

For more information about the NASA STI Program Office, see the following:

- Access the NASA STI Program Home Page at ***http://www.sti.nasa.gov***

- E-mail your question via the Internet to help@sti.nasa.gov

- Fax your question to the NASA Access Help Desk at (301) 621–0134

- Telephone the NASA Access Help Desk at (301) 621–0390

- Write to:
  NASA Access Help Desk
  NASA Center for AeroSpace Information
  7121 Standard Drive
  Hanover, MD 21076–1320
  (301)621–0390

NASA/TM—2004–213282

Solid Rocket Booster Hydraulic Pump Port Cap Joint Load Testing

W.R. Gamwell and N.C. Murphy
Marshall Space Flight Center, Marshall Space Flight Center, Alabama

National Aeronautics and
Space Administration

Marshall Space Flight Center • MSFC, Alabama 35812

June 2004

Acknowledgments

The authors would like to acknowledge the assistance of those individuals who aided in the preparation of this document. Testing was conducted by Mr. James Hodo of the Marshall Space Flight Center Mechanical Metallurgy and Corrosion Engineering Team. This publication was originally formatted and edited by Mrs. Susan Hessler of Morgan Research Corporation.

TRADEMARKS

Available from:

NASA Center for AeroSpace Information
7121 Standard Drive
Hanover, MD 21076–1320
(301) 621–0390

National Technical Information Service
5285 Port Royal Road
Springfield, VA 22161
(703) 487–4650

TABLE OF CONTENTS

LIST OF FIGURES

LIST OF FIGURES (Continued)

LIST OF FIGURES (Continued)

LIST OF TABLES

LIST OF ACRONYMS

CA	corrosion-resistent steel type A286
DMX	maximum displacement in inches
DOF	degrees of freedom
FEM	finite element model
MN	minimum
MS	military standard
MX	maximum
PH	precipitation hardening
SMN	minimum stress in pounds per square inch
SMX	maximum stress in pounds per square inch

NOMENCLATURE

A_{ah}	area of aluminum housing in compression
A_b	bolt cross-sectional area
A_{pc}	area of port cap in compression
A_{sp}	area of spacer washer in compression
E_{ah}	elastic modulus of aluminum housing
E_b	elastic modulus of bolt
E_{pc}	elastic modulus of port cap
E_{sp}	elastic modulus of spacer washer
F_b	change in bolt load
F_e	applied external force
F_i	initial load in bolt from preload torque
F_t	bolt load
k_{ah}	stiffness of aluminum housing
k_b	bolt stiffness
k_c	stiffness of compressed parts in series
k_{pc}	stiffness of port cap
k_{sp}	stiffness of spacer washer
L_{ah}	thickness of aluminum housing
L_b	length of bolt
L_{pc}	thickness of port cap
L_{sp}	thickness of spacer washer

TECHNICAL MEMORANDUM

SOLID ROCKET BOOSTER HYDRAULIC PUMP PORT CAP JOINT LOAD TESTING

1. INTRODUCTION

The solid rocket booster uses pumps to provide hydraulic fluid to the aft skirt thrust vector control system. At present, these hydraulic pumps are fabricated from cast C355 aluminum alloy, with pump port caps fabricated from 17–4 precipitation-hardening (PH) stainless steel. Corrosion-resistant steel, MS51830 CA 204L self-locking screw thread inserts are installed into the C355 pump housings and A286 stainless steel fasteners are installed into the inserts to secure the pump port cap to the pump housing.

In the past, the A286 hydraulic pump port cap fasteners were installed to an installation torque of 33 Nm (300 in-lb). However, it was determined that the structural analyses had used a significantly higher nut factor than the one indicated by tests conducted by Boeing Space Systems in Huntington Beach, CA. A reassessment of the original design torque values was made using Boeing's lower nut factor, which revealed a factor of safety of <1 for fastener preload with the potential for overloading the hydraulic pump port cap joint. This analysis was supported by subsequent hardware inspections. Six pumps were found to have the insert pulled up to flush or above flush to the backside of the pump port cap due to shearing of tapped aluminum threads in the pump housings.

Lower torque limits were established at 14.3 to 19.8 Nm (130 to 180 in-lb) for pump port cap fasteners. This change required delta-qualification tests to recertify the pumps. A new requirement was also added to limit insert axial deformation to 0.008 cm (0.003 in) under operating conditions after an initial preload was applied to seat the insert.

2. TECHNICAL APPROACH

Testing was performed by the Marshall Space Flight Center Materials, Processes, and Manufacturing Department in order to support an understanding of the hydraulic pump insert deformation at the reduced preload with an external applied load, along with port cap-to-housing joint stiffness characteristics. This study used a simulated hydraulic pump port cap-to-housing joint configuration. Tests were conducted to determine whether the insert would move axially when a bolt preload plus an external axial load were applied to the joint, as well as to determine changes in the bolt preload when external loads were applied.

3. EXPERIMENTAL PROCEDURES

3.1 Test Setup

The following equipment and materials were used to conduct these tests:

- A 50-kN (10-kip) mechanical testing load frame with computer control software (fig. 1).
- A standard steel fastener test fixture cage to accommodate an A286 stainless steel Strainsert bolt (fig. 2).
- A 6061–T6 aluminum test cylinder with a 0.952-cm (0.375-in) MS51830 CA 204L self-locking insert installed to simulate the pump port cap insert configuration (fig. 3).
- A 17–4 PH stainless steel drop-through fixture to simulate the pump port cap material and thickness (fig. 4).
- Strainsert bolts to determine load in the joint (fig. 5).
- A hardened 4340 bearing steel spacer to accommodate the Strainsert bolts which were longer than the flight bolts (fig. 6).
- Strain conditioners to determine loads in the Strainsert bolt.

3.2 Pretest Procedure

The following procedure was used to make preparations for these tests:

(3.2.1) Verify calibration of Strainsert bolt.

(3.2.2) Install standard steel fastener test fixture into load frame. Axially align and verify alignment.

(3.2.3) Install Strainsert bolt into a load frame using a standard steel fastener test fixture cage, the drop-through fixture, the spacer, and the clevis (fig. 7).

(3.2.4) Load Strainsert bolt to 2,268 kg (5,000 lb).

(3.2.5) Compare load in bolt to applied load from frame.

(3.2.6) Resolve any calibration issues prior to starting joint test.

(3.2.7) Verify depth of the top of the insert below the top of the clevis.

(3.2.8) Mark clevis with two reference lines, perpendicular to each other and centered on the insert. Identify the four locations that intersect the insert (fig. 8).

(3.2.9) Measure and record insert depth using a depth caliper with a stabilizing bottom support (fig. 9).

(3.2.10) Measure depth at four locations 90° apart (as marked by reference lines) three times each.

(3.2.11) Record measurements by location.

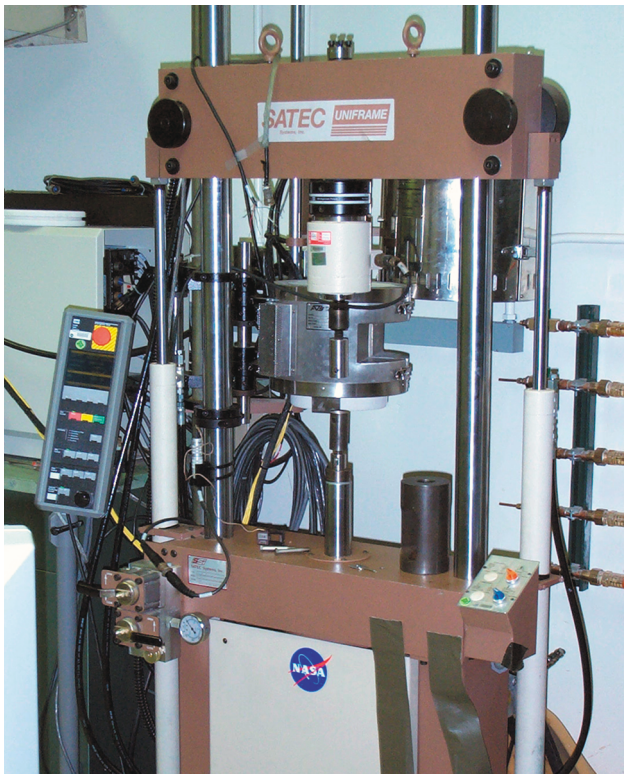

Figure 1. Mechanical testing load frame.

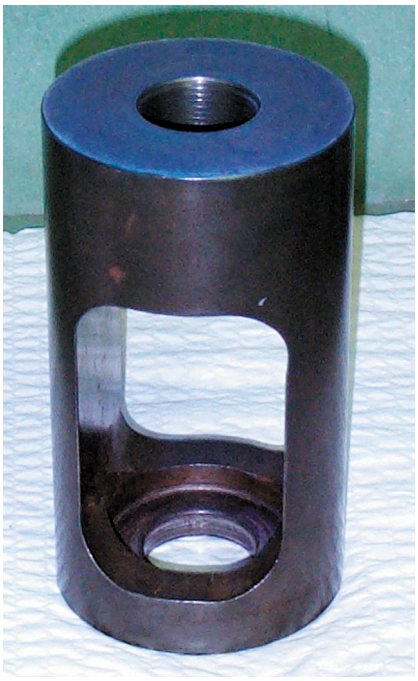

Figure 2. Standard steel fastener test fixture.

Figure 3. 6061–T6 aluminum test cylinder with 0.952-cm (0.375-in) Keensert® thread insert.

Figure 4. 17–4 PH stainless steel drop-through fixture.

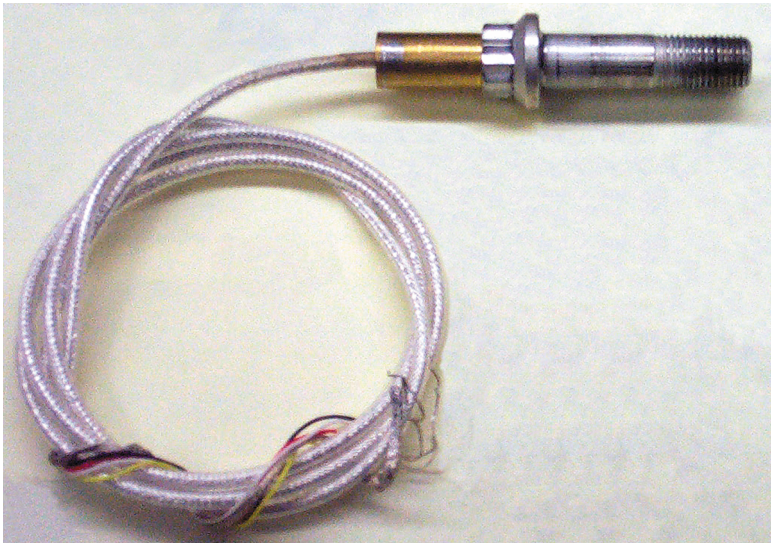

Figure 5. A286 stainless steel Strainsert (long bolt).

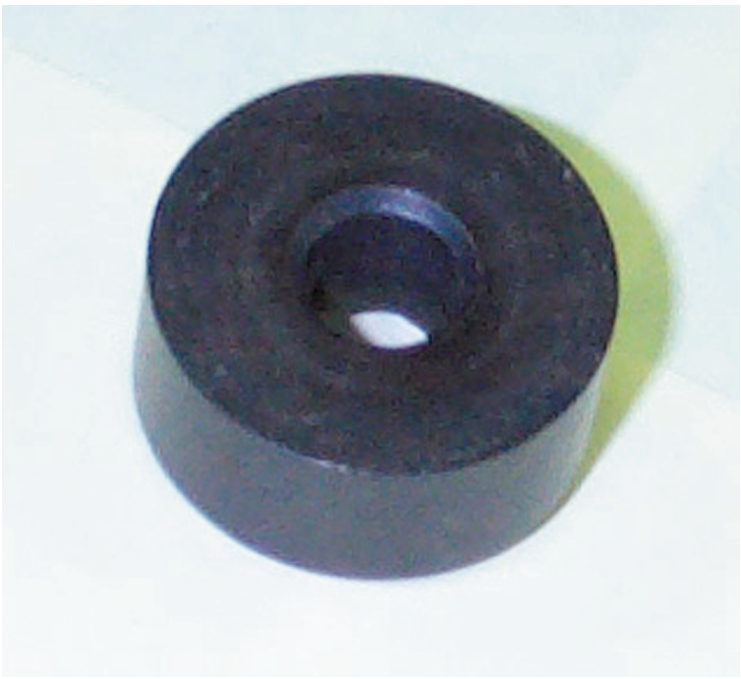

Figure 6. Hardened 4340 bearing steel spacer used in test setup (long bolt).

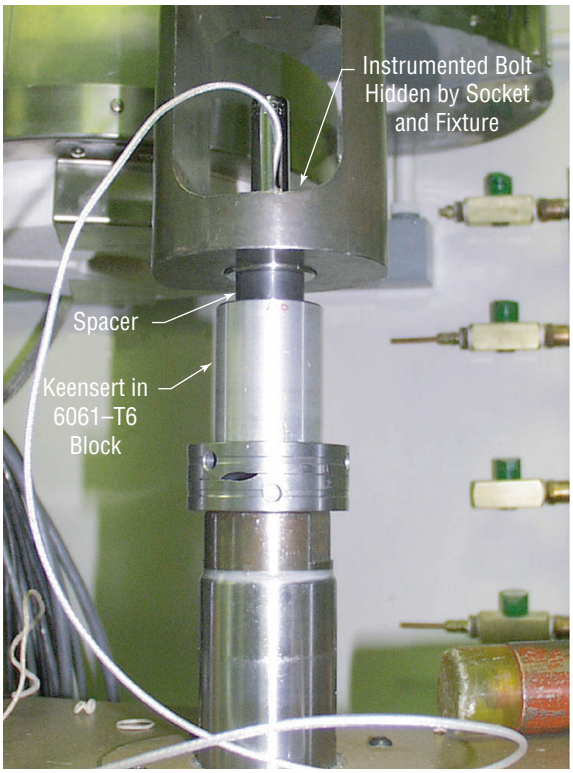

Figure 7. Load frame with test setup (long bolt).

Figure 8. Scribe lines identifying locations where test cylinder intersected insert.

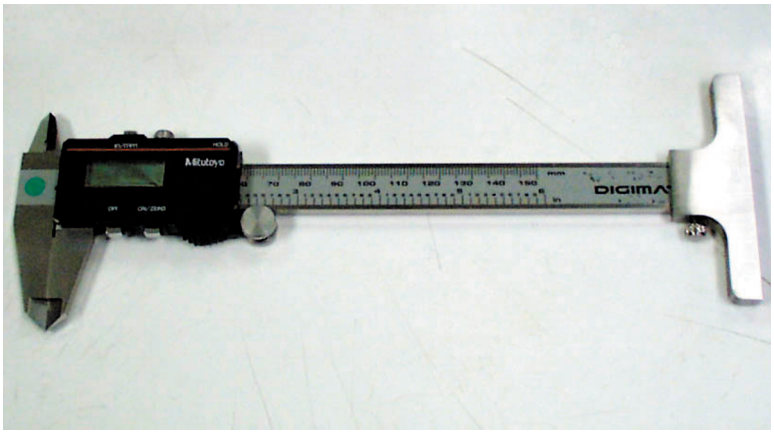

Figure 9. Calipers with stabilizing bottom support.

3.3 Test Procedure for Cap Bolt/Insert Joint

The following procedure was used to conduct these tests:

(3.3.1) Install fixture, axially align, and verify alignment for 17–4 PH stainless steel/6061–T6 aluminum joint.

(3.3.2) Install Strainsert bolt and preload to a maximum load of 726 kg (1,600 lb). Load in increments of 5.5 Nm (50 in-lb). Hold for 5 min.

(3.3.3) Remove bolt and conduct depth measurements (as specified in 3.2.9 through 3.2.11).

(3.3.4) Reinstall Strainsert bolt and preload to a maximum load of 862 kg (1,900 lb). Load in increments of 5.5 Nm (50 in-lb). Hold for 5 min.

(3.3.5) Apply external load of 363 kg (800 lb) to the joint using load frame.

(3.3.6) Record applied load and the load in the Strainsert bolt simultaneously during loading.

(3.3.7) Remove bolt and conduct depth measurements.

(3.3.8) Reinstall Strainsert bolt and preload to a maximum load of 862 kg (1,900 lb). Load in increments of 5.5 Nm (50 in-lb). Hold for 5 min.

(3.3.9) Apply 726-kg (1,600-lb) external load to the joint using load frame.

(3.3.10) Record applied load and the load in the Strainsert bolt simultaneously during loading.

(3.3.11) Remove bolt and conduct depth measurements.

(3.3.12) Reinstall Strainsert bolt and preload to a maximum load of 862 kg (1,900 lb). Load in increments of 5.5 Nm (50 in-lb). Hold for 5 min.

(3.3.13) Apply 1,089-kg (2,400-lb) external load to the joint using load frame.

(3.3.14) Record applied load and the load in the Strainsert bolt simultaneously during loading.

(3.3.15) Remove bolt and conduct depth measurements.

(3.3.16) Reinstall Strainsert bolt and preload to a maximum load of 2,404 kg (5,300 lb) (maximum preload). Load in increments of 5.5 Nm (50 in-lb). Hold for 5 min.

(3.3.17) Apply 363-kg (800-lb) external load to the joint using load frame.

(3.3.18) Record applied load and the load in the Strainsert bolt simultaneously during loading.

(3.3.19) Remove bolt and conduct depth measurements.

(3.3.20) Reinstall Strainsert bolt and preload to a maximum load of 2,404 kg (5,300 lb) (maximum preload). Load in increments of 5.5 Nm (50 in-lb). Hold for 5 min.

(3.3.21) Apply 726-kg (1,600-lb) external load to the joint using load frame.

(3.3.22) Record applied load and the load in the Strainsert bolt simultaneously during loading.

(3.3.23) Remove bolt and conduct depth measurements.

(3.3.24) Reinstall Strainsert bolt and preload to a maximum load of 2,404 kg (5,300 lb) (maximum preload). Load in increments of 5.5 Nm (50 in-lb). Hold for 5 min.

(3.3.25) Apply 1,089-kg (2,400-lb) external load to the joint using load frame.

(3.3.26) Record applied load and the load in the Strainsert bolt simultaneously during loading.

(3.3.27) Remove bolt and conduct depth measurements.

(3.3.28) Reinstall Strainsert bolt and preload to a maximum load of 1,633 kg (3,600 lb) load in increments of 5.5 Nm (50 in-lb). Hold for 5 min.

(3.3.29) Apply 1,089 kg (2,400 lb) external load to the joint using load frame.

(3.3.30) Record applied load and the load in the Strainsert bolt simultaneously during loading.

(3.3.31) Remove bolt.

4. RESULTS AND DISCUSSION

4.1 Clevis with Insert Depth Measurements

Table 1 shows depth measurements for the top of the insert below the surface of the clevis, which were taken prior to testing and after various bolt preload plus external load applications. After any combination of bolt preload plus external loading, the maximum axial movement exhibited from the top of the insert toward the top of the clevis was 3.5 mil (88.9 μm or 0.0035 in), which occurred at the 90° measurement locations. Depth was defined as the average of all 12 measurements, due to variations seen at individual locations. By this definition, the starting pretest depth was 0.0287 cm (0.0113 in) and the maximum change was 2 mil (50.8 μm or 0.002 in), including a change of 0.4 mil (10.16 μm or 0.0004 in) from the initial seating preload of 726 kg (1,600 lb). These findings were within the allowable movement established for the pump delta-qualification program.

4.2 Preload and External Load

Figures 10 through 28 show results for preload, external load, and preload plus external load. Figures 11 through 13 show that the change in bolt load versus the applied external load increased in a nonlinear fashion, with increasing external load for the low preload case of 862 kg (1,900 lb) and medium preload case of 1,633 kg (3,600 lb). The change in bolt load for the high preload case of 2,404 kg (5,300 lb) was linear to ≈680 kg (1,500 lb) of applied external load before becoming nonlinear.

Table 2 and figure 29 show the effect of various external loads on the initial preload conditions. Generally the change in bolt load was small compared to the external loads applied to the joint. This result indicates that the stiffness of the compressed parts, the port cap and housing, was less than the bolt stiffness. Bolt loads increased as the external loads increased. The change in bolt load was lower for the high initial preload case when similar external loads were applied.

Table 1. Depth measurements and results (in inches) for top of insert below clevis surface (long bolt).

	Test 1	Test 2	Test 3	Average
Before testing				
0˚	0.0105	0.0105	0.0105	0.0105
90˚	0.0115	0.0100	0.0115	0.0110
180˚	0.0120	0.0125	0.0125	0.0123
270˚	0.0115	0.0115	0.0115	0.0115
1,600-lb preload and 5-min hold				
0˚	0.0100	0.0105	0.0100	0.0102
90˚	0.0105	0.0105	0.0105	0.0105
180˚	0.0120	0.0105	0.0120	0.0115
270˚	0.0115	0.0115	0.0115	0.0115
1,900-lb preload and 5-min hold; 800-lb external load				
0˚	0.0080	0.0080	0.0085	0.0082
90˚	0.0095	0.0090	0.0095	0.0093
180˚	0.0115	0.0115	0.0110	0.0113
270˚	0.0100	0.0100	0.0100	0.0100
1,900-lb preload and 5-min hold; 1,600-lb external load				
0˚	0.0085	0.0085	0.0085	0.0085
90˚	0.0095	0.0090	0.0090	0.0092
180˚	0.0110	0.0110	0.0110	0.0110
270˚	0.0100	0.0100	0.0100	0.0100
1,900-lb preload and 5-min hold; 2,400-lb external load				
0˚	0.0085	0.0085	0.0085	0.0085
90˚	0.0095	0.0095	0.0095	0.0095
180˚	0.0110	0.0110	0.0110	0.0110
270˚	0.0100	0.0100	0.0105	0.0102
5,300-lb preload and 5-min hold; 800-lb external load				
0˚	0.0090	0.0090	0.0090	0.0090
90˚	0.0100	0.0100	0.0100	0.0100
180˚	0.0115	0.0115	0.0115	0.0115
270˚	0.0105	0.0105	0.0105	0.0105
5,300-lb preload and 5-min hold; 1,600-lb external load				
0˚	0.0085	0.0085	0.0085	0.0085
90˚	0.0080	0.0090	0.0095	0.0088
180˚	0.0110	0.0105	0.0110	0.0108
270˚	0.0100	0.0100	0.0100	0.0100
5,300-lb preload and 5-min hold; 2,400-lb external load				
0˚	0.0085	0.0090	0.0085	0.0087
90˚	0.0095	0.0100	0.0095	0.0097
180˚	0.0110	0.0110	0.0110	0.0110
270˚	0.0100	0.0100	0.0100	0.0100

Table 1. Depth measurements and results (in inches) for top of insert below clevis surface (long bolt) (continued).

Summary of Insert Results				
	Before	After	Average	Maximum
0˚	0.0105	0.0082	0.0023	0.0025
90˚	0.0110	0.0088	0.0022	0.0035
180˚	0.0123	0.0108	0.0015	0.0020
270˚	0.0115	0.0100	0.0015	0.0015

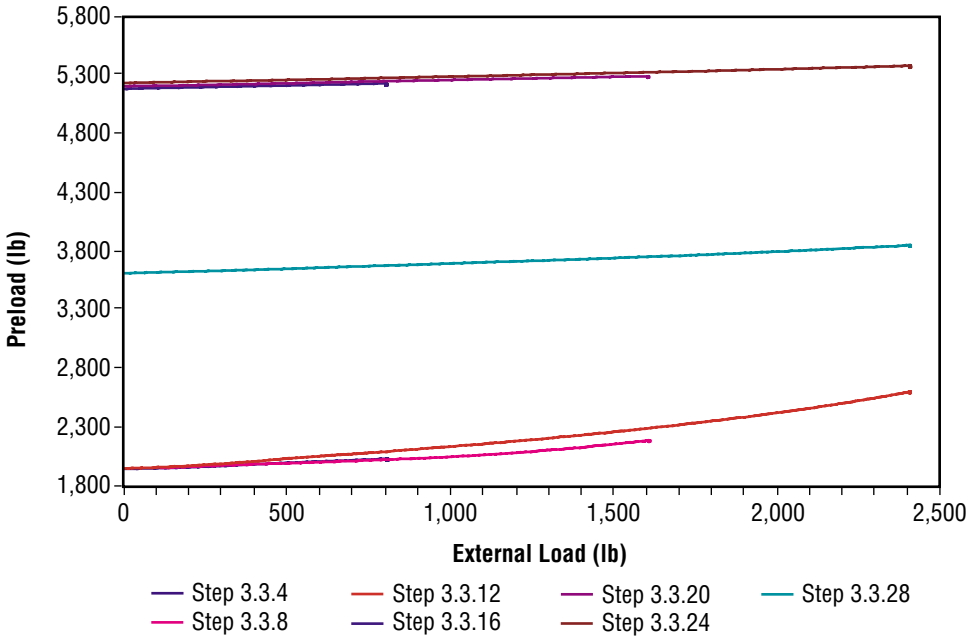

Figure 10. Preload versus external load results (long bolt).

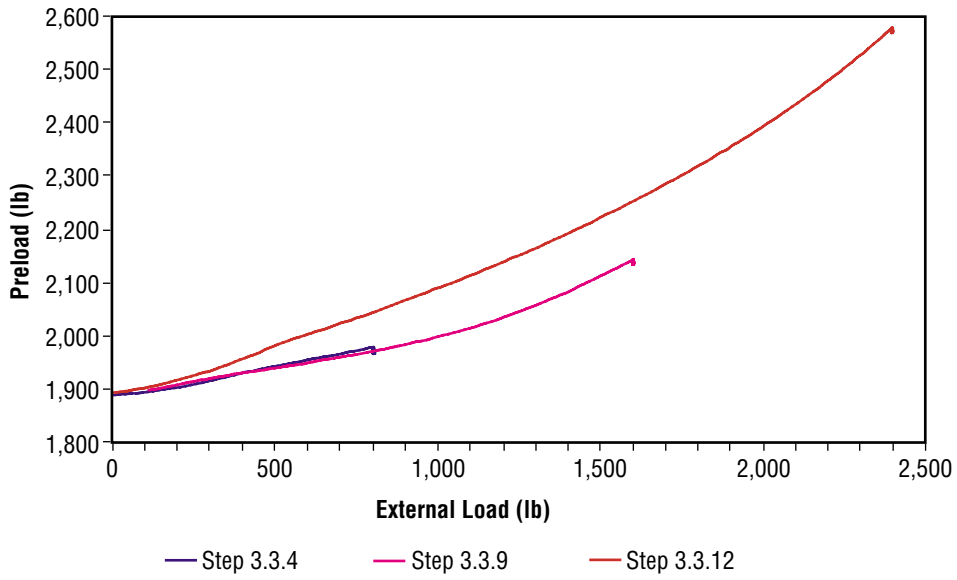

Figure 11. Effects of low preload of 862 kg (1,900 lb) with external loads of 363, 726, and 1,089 kg (800, 1600, and 2,400 lb) for long bolt.

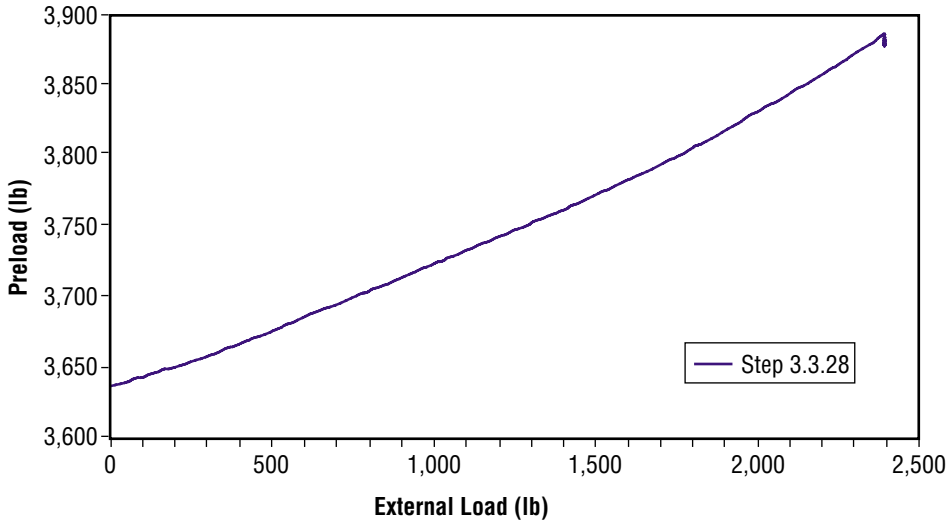

Figure 12. Change in initial load for medium preload of 1,633 kg (3,600 lb) with external load of 1,089 kg (2,400 lb) for long bolt.

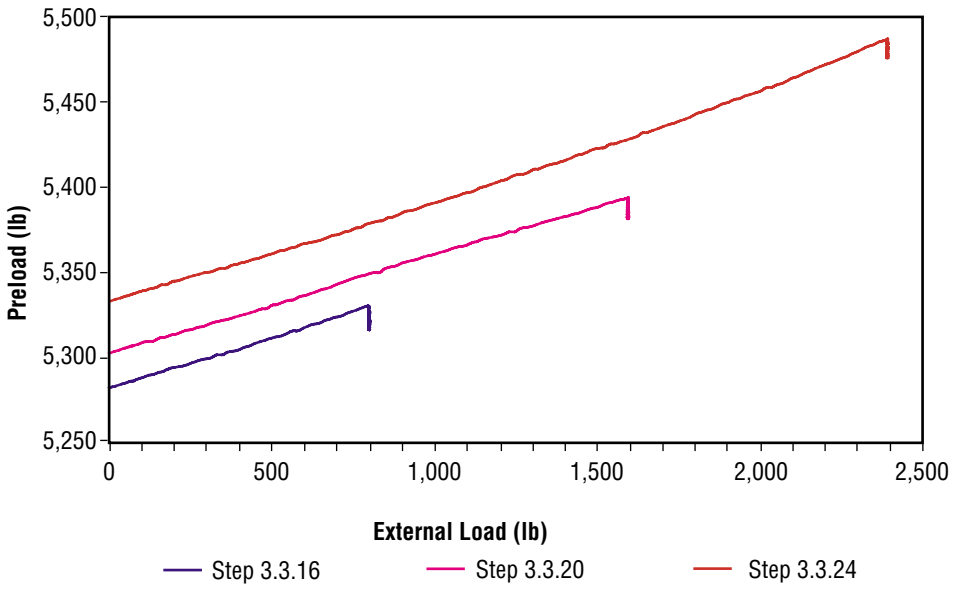

Figure 13. Effects of high preload of 2,404 kg (5,300 lb) with external loads of 363, 726, and 1,089 kg (800, 1,600, and 2,400 lb) for long bolt.

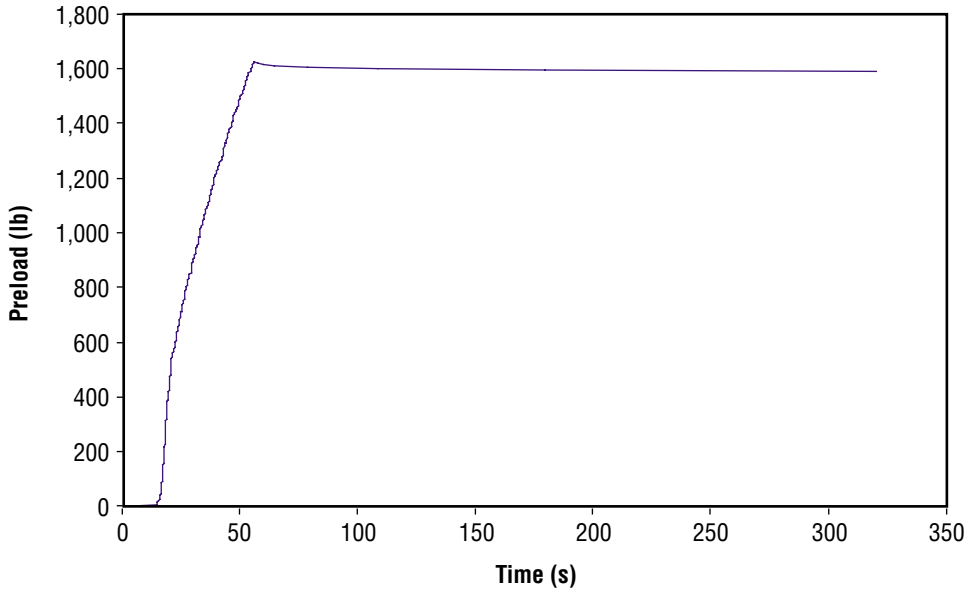

Figure 14. Step 3.3.2 results for preload of 726 kg (1,600 lb) for long bolt.

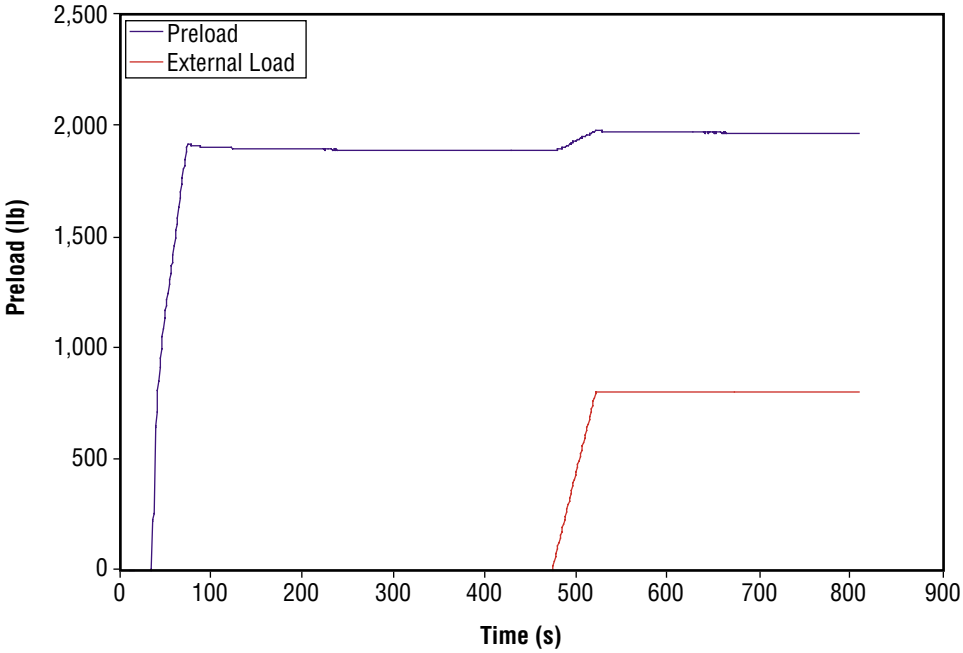

Figure 15. Step 3.3.4 results for preload of 862 kg (1,900 lb) with external load of 363 kg (800 lb) for long bolt.

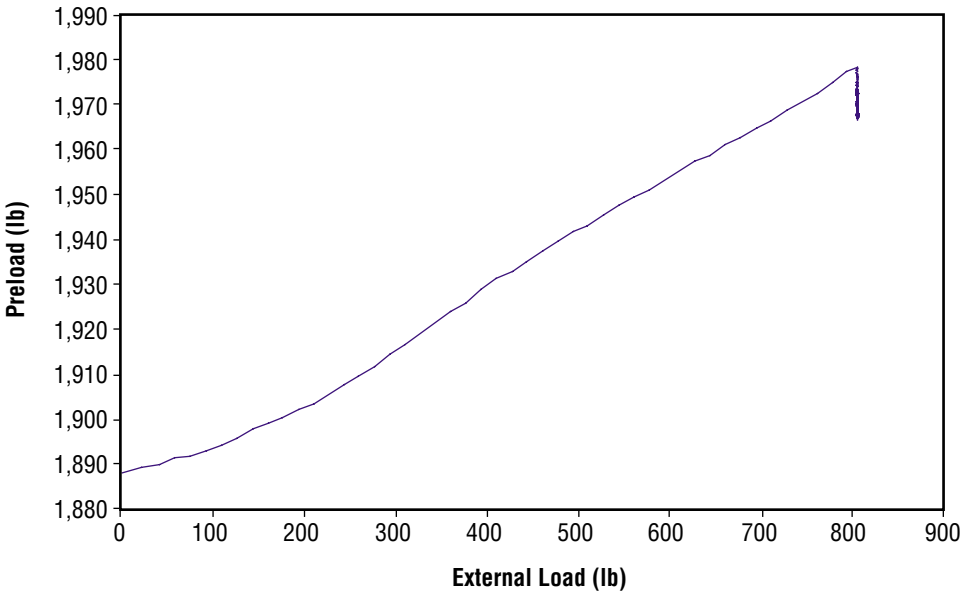

Figure 16. Step 3.3.4 results for preload of 862 kg (1,900 lb) versus external load of 363 kg (800 lb) for long bolt.

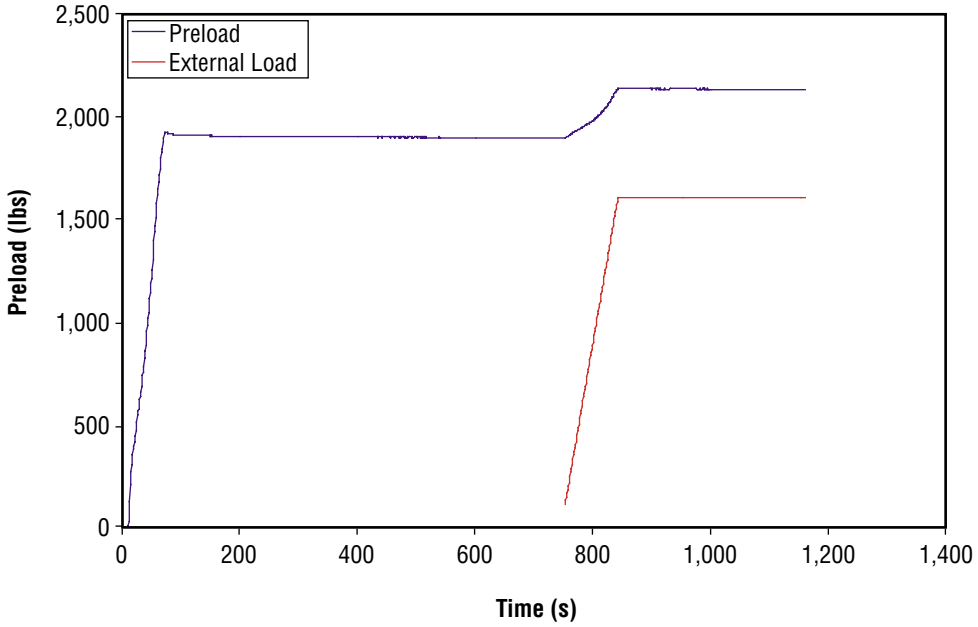

Figure 17. Step 3.3.8 results for preload of 862 kg (1,900 lb) with external load of 726 kg (1,600 lb) for long bolt.

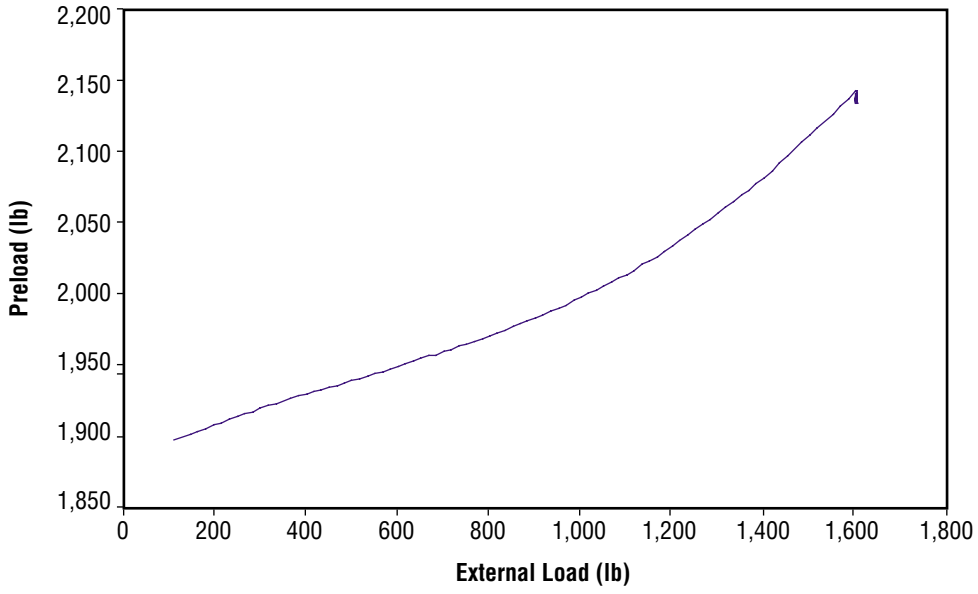

Figure 18. Step 3.3.8 results for preload of 862 kg (1,900 lb) versus external load of 726 kg (1,600 lb) for long bolt.

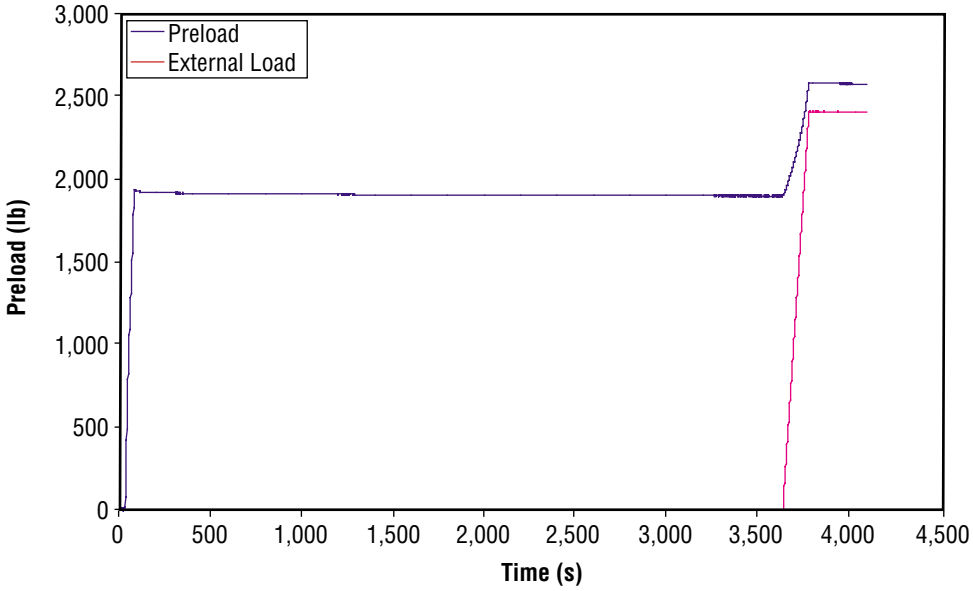

Figure 19. Step 3.3.12 results for preload of 862 kg (1,900 lb) with external load of 1,089 kg (2,400 lb) for long bolt.

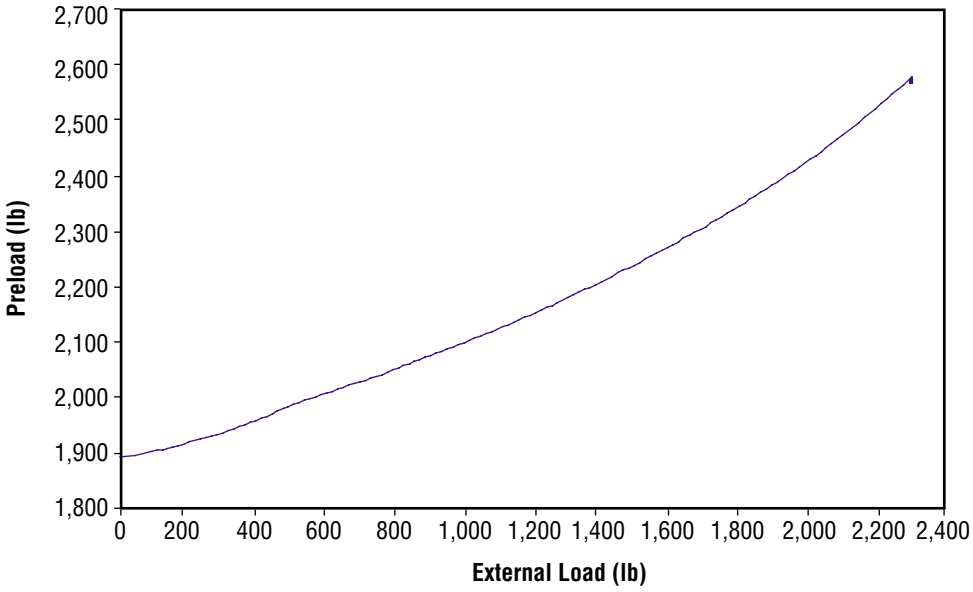

Figure 20. Step 3.3.12 results for preload of 862 kg (1,900 lb) versus external load of 1,089 kg (2,400 lb) for long bolt.

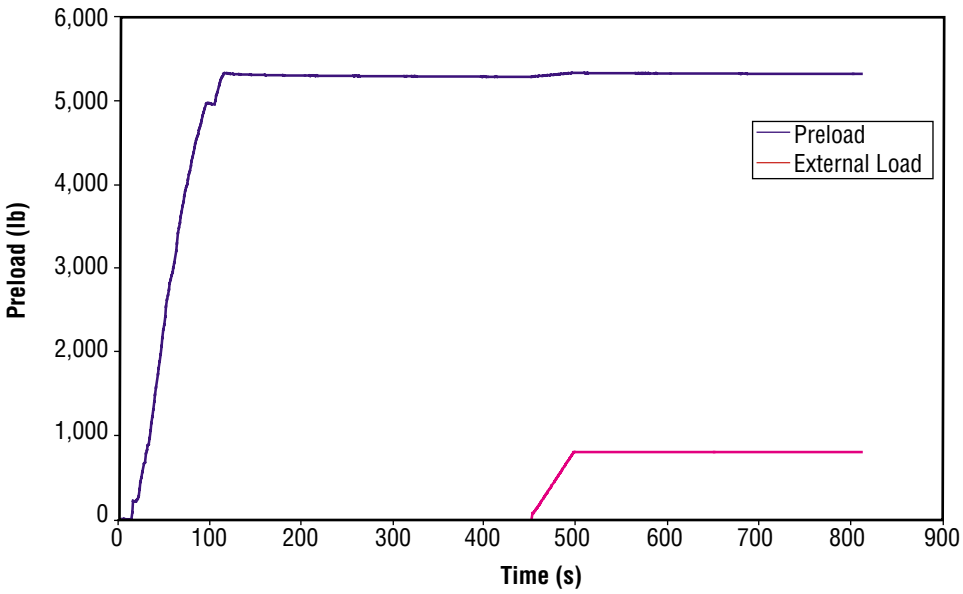

Figure 21. Step 3.3.16 results for preload of 2,404 kg (5,300 lb) with external load of 363 kg (800 lb) for long bolt.

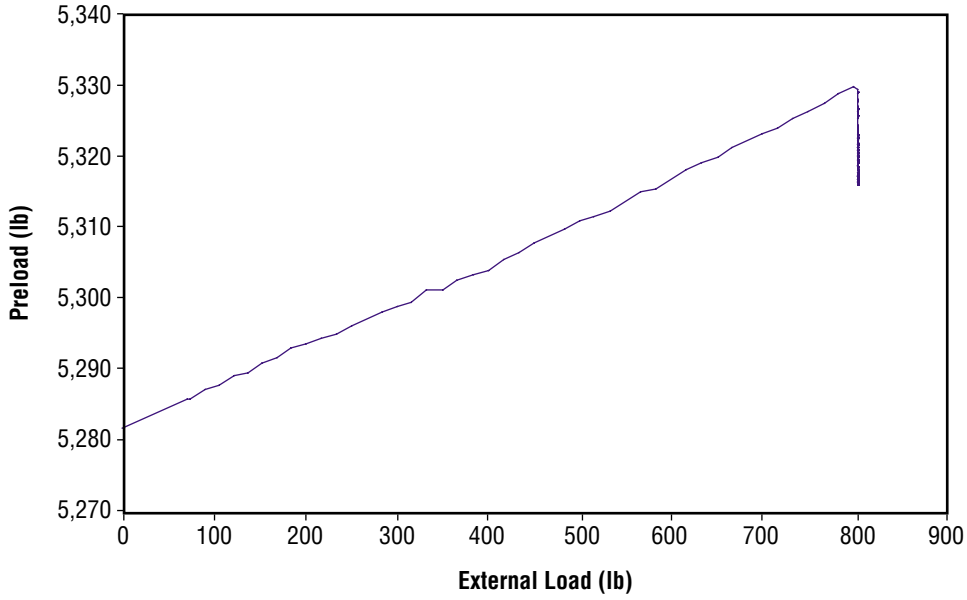

Figure 22. Step 3.3.16 results for preload of 2,404 kg (5,300 lb) versus external load of 363 kg (800 lb) for long bolt.

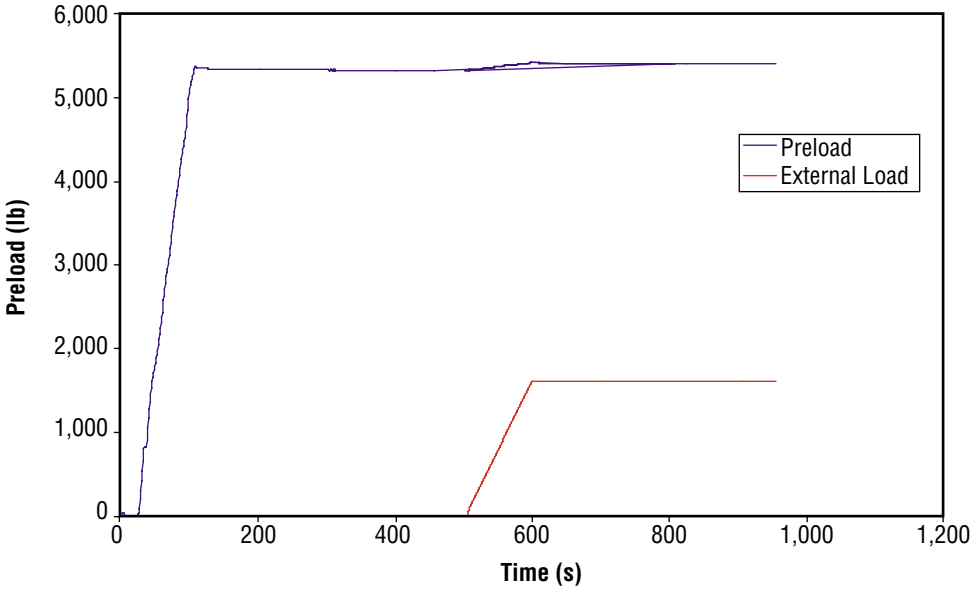

Figure 23. Step 3.3.20 results for preload of 2,404 kg (5,300 lb) with external load of 726 kg (1,600 lb) for long bolt.

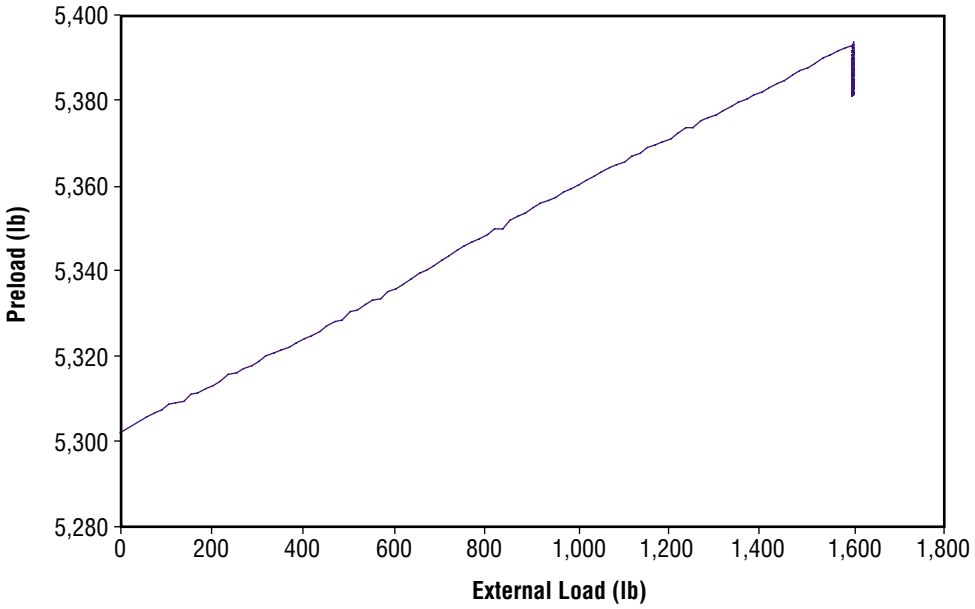

Figure 24. Step 3.3.20 results for preload of 2,404 kg (5,300 lb) versus external load of 726 kg (1,600 lb) for long bolt.

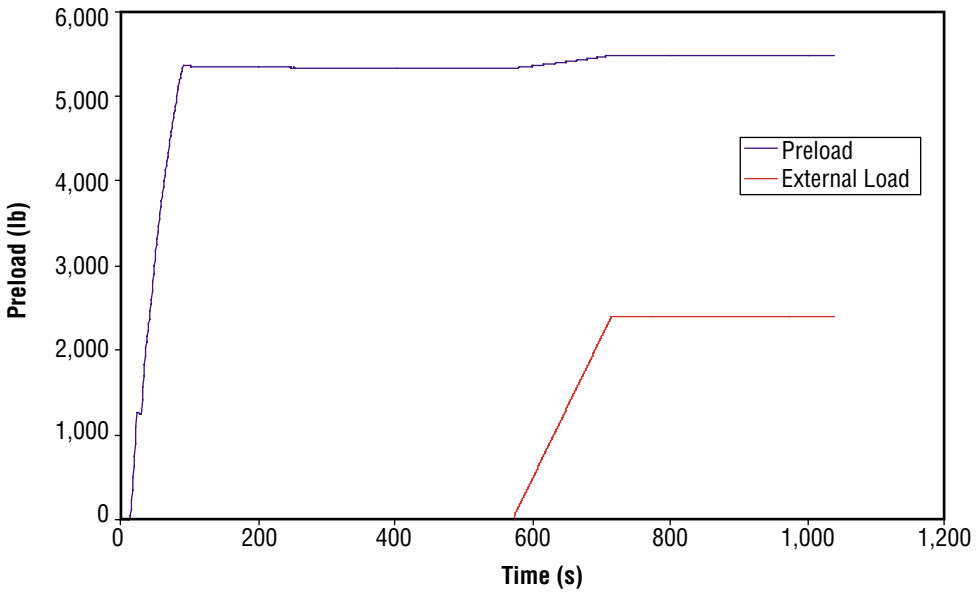

Figure 25. Step 3.3.24 results for preload of 2,404 kg (5,300 lb) with external load of 1,089 kg (2,400 lb) for long bolt.

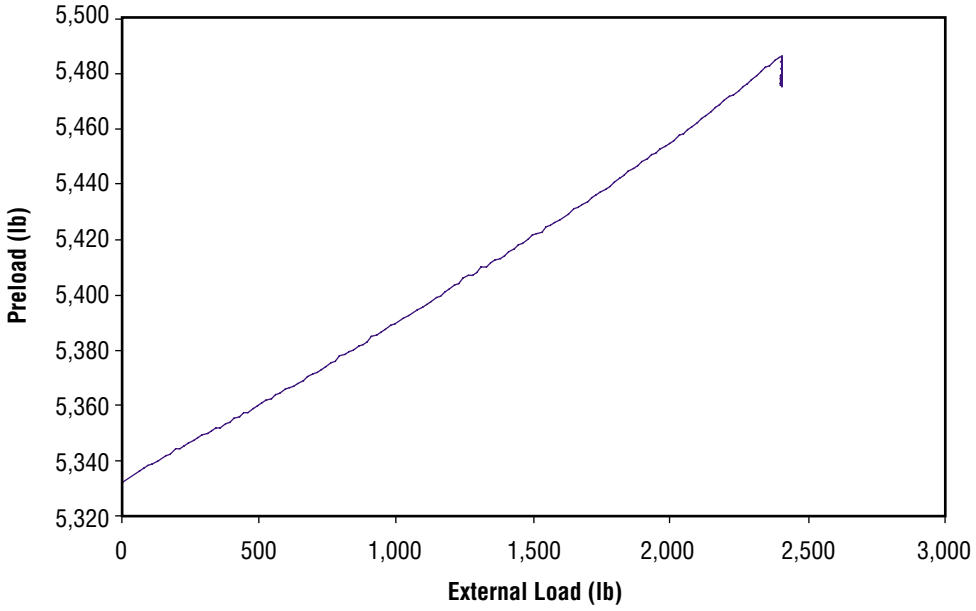

Figure 26. Step 3.3.24 results for preload of 2404 kg (5,300 lb) versus external load of 1,089 kg (2,400 lb) for long bolt.

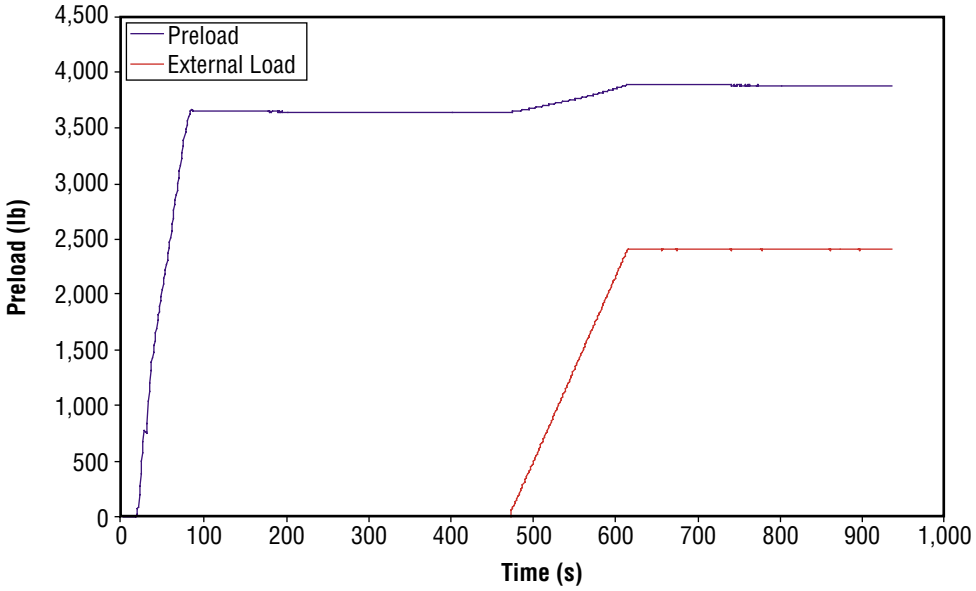

Figure 27. Step 3.3.28 results for preload of 1,633 kg (3,600 lb) with external load of 1,089 kg (2,400 lb) for long bolt.

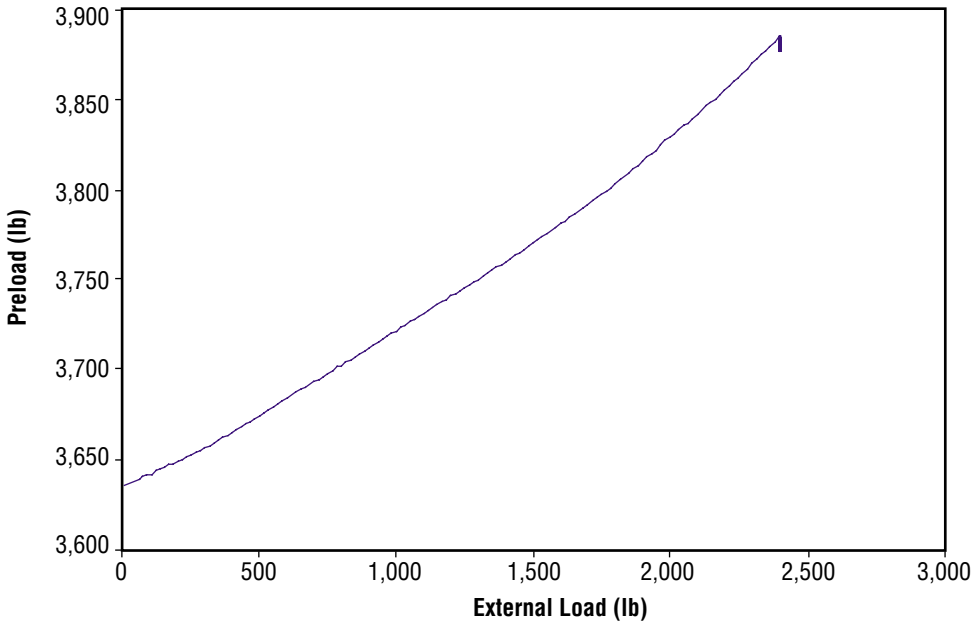

Figure 28. Step 3.3.28 results for preload of 1,633 kg (3,600 lb) versus external load of 1,089 kg (2,400 lb) for long bolt.

Table 2. Change in initial loads for preloads of 862, 1,633, and 2,404 kg (1,900, 3,600, and 5,300 lb) versus external loads of 363, 726, and 1089 kg (800, 1,600, and 2,400 lb) for long bolt.

Bolt Preload (lb)	Applied External Load (lb)	Change in Bolt Load (lb)	Delta (lb)
1,900	800	1,888–1,978	90
1,900	1,600	1,898–2,142	244
1,900	2,400	1,893–2,577	684
3,600	2,400	3,635–3,885	250
5,300	800	5,282–5,330	48
5,300	1,600	5,302–5,393	91
5,300	2,400	5,332–5,487	155

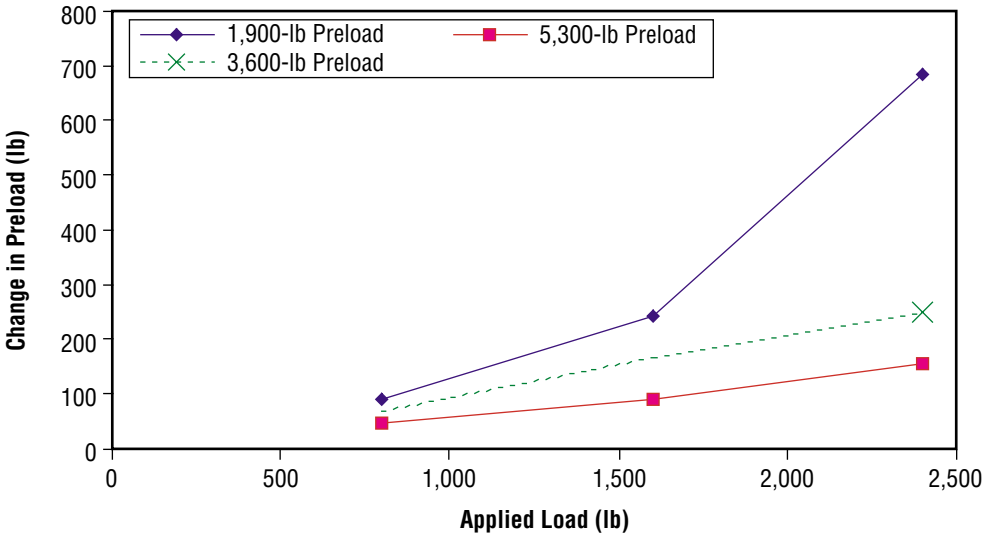

Figure 29. Change in initial loads for preloads of 862, 1,633, and 2,404 kg (1,900, 3,600, and 5,300 lb) versus external loads of 363, 726, and 1,089 kg (800, 1,600, and 2,400 lb) for long bolt.

4.3 Finite Element Model Analysis

ANSYS® software was used to make a finite element model (FEM) to evaluate the behavior of a preloaded joint with self-locking screw thread inserts. Figures 30 and 31 show two-dimensional axisymmetric FEMs for the test configuration and forces applied to it, respectively. Table 3 lists material properties used in the FEM.

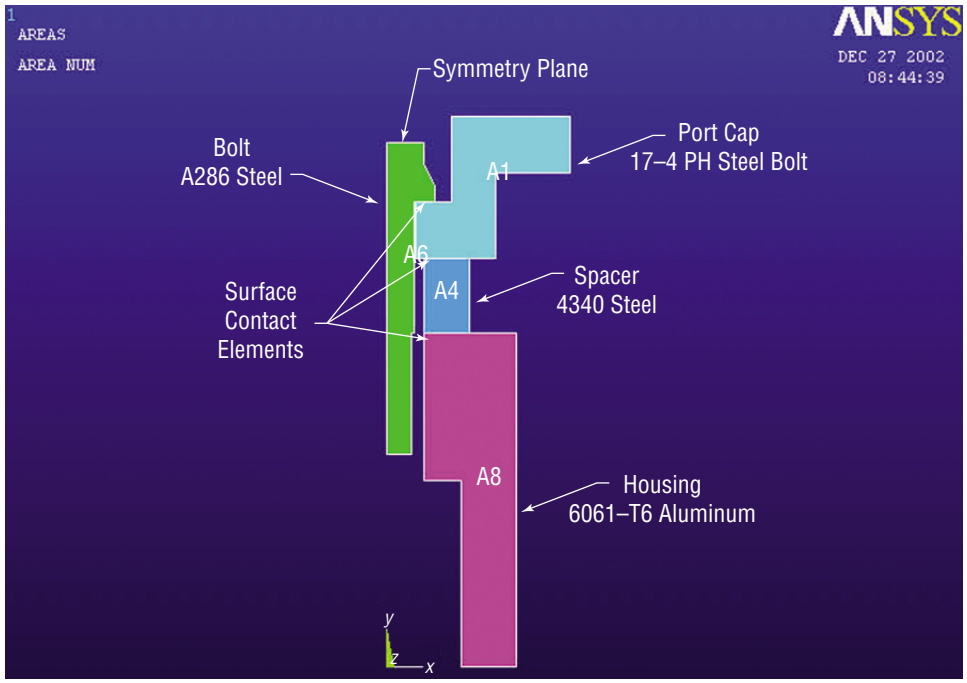

Figure 30. FEM for test configuration (long bolt).

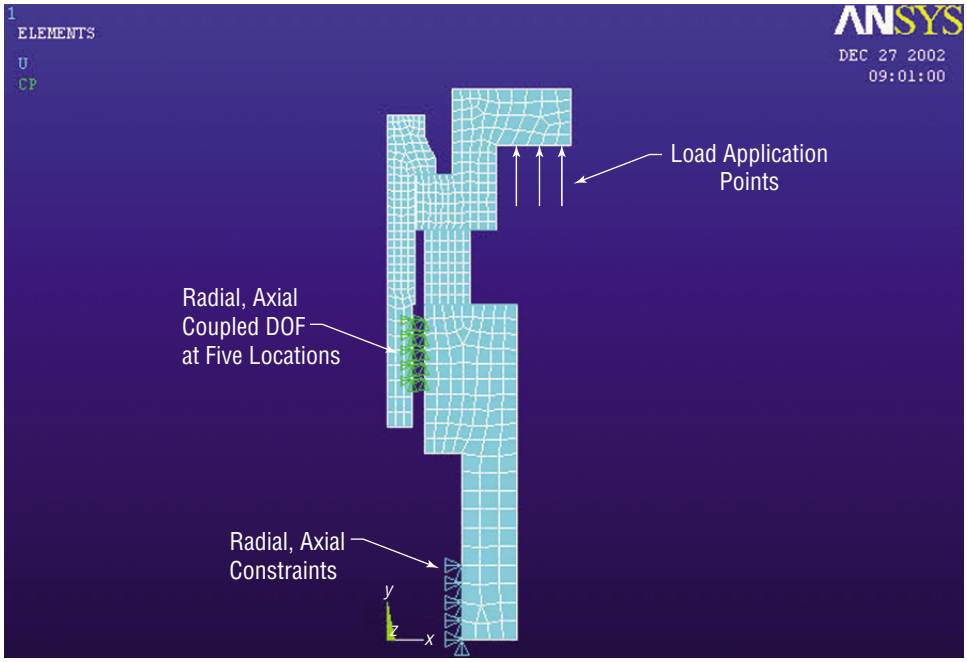

Figure 31. FEM for forces applied to test configuration (long bolt).

Table 3. Material properties used for FEM analysis.

Item	Material	Modulus (psi)	Poisson's Ratio
Bolt	A286 stainless steel	29.0×10^6	0.33
Port cap	17–4 PH stainless steel	28.5×10^6	0.28
Housing	6061–T6 aluminum	10.3×10^6	0.33
Spacer	4340 bearing steel	29.0×10^6	0.33

Each part was modeled discretely, with contact elements under the bolt head and between the port cap, spacer, and housing. The contact elements allowed compression forces to be transmitted only between parts. These elements were also used to develop the bolt preload by specifying an initial interference between the bolt head and port cap. The load transfer between bolt threads and the housing was achieved by coupling the radial and axial degrees of freedom at the five thread interface nodes. After achieving an initial state of preload with the desired bolt tension, the external forces were applied in increments of 113 to 227 kg (250 to 500 lb). The increase in bolt tension was calculated and saved at each load step until all compression contact was relieved between the port cap and housing.

Typically, hand analysis methods are used to calculate the change in bolt load in a preloaded joint that experiences applied external forces which try to gap the connection. The derivation of the following equations was obtained from *Design of Machine Elements*:[1]

F_t = bolt load = $F_i + F_b$;

F_i = initial load in bolt from preload torque;

F_b = change in bolt load = $(k_b/(k_b + k_c))F_e$, where F_e is the applied external force;

k_b = bolt stiffness = $A_b E_b/L_b$, using the bolt cross-sectional area, elastic modulus, and length;

k_c = stiffness of the compressed parts in series, $1/k_c = 1/k_{pc} + 1/k_{ah} + 1/k_{sp}$;

k_{pc} = stiffness of the port cap = $A_{pc}E_{pc}/L_{pc}$, using an estimate of the area in compression, elastic modulus, and thickness of the port cap;

k_{ah} = stiffness of the aluminum housing = $A_{ah}E_{ah}/L_{ah}$, using an estimate of the area in compression, elastic modulus, and thickness of the aluminum housing; and

k_{sp} = stiffness of the spacer washer = $A_{sp}E_{sp}/L_{sp}$, using an estimate of the area in compression, elastic modulus, and thickness of the washer used as a spacer to accommodate the bolt that was longer than the flight configuration by ≈1.3 cm (0.5 in).

When using textbook methods to calculate F_b, assumptions must be made on five parameters ($L_b, A_{pc}, A_{ah}, L_{ah}, A_{sp}$). As a result, F_b varies anywhere from $0.08F_e$ to $0.3F_e$, which can lead to a significant overprediction of bolt load or an underprediction of the load at which the joint gaps. These equations also assume that the change in bolt load will vary in a linear fashion until preload compression is overcome in the joint.

The test results showed that the change in bolt load was generally much less than expected and predominately nonlinear as a function of applied external load. FEM analysis was used to gain an understanding of these results. Although lower than the test values, the FEM confirmed that the slope of the bolt load change for this type of joint was less than might be expected using textbook solutions. Figure 32 shows the change in bolt load for three starting preloads. Figures 33 and 34 show typical distributions for axial stress and contact surface pressure. Table 4 compares FEM and test percent change in bolt load for the three preload cases evaluated.

FEM did not exhibit the nonlinear behavior shown by test results for bolt load versus applied load curve, except the preload of 862 kg (1,900 lb) beyond an applied load of 567 kg (1,250 lb). A possible explanation for the nonlinear curve was found in the FEM compressive stress zones and the nonlinear nature of the contact pressure distribution, which was concentrated around the bolt hole.

Table 4. Percent change in bolt load for FEM versus test data.

Preload	Test (%)	FEM (%)
≈862 kg (1,900 lb)	10 to 20	6.2 to 12.7
≈1,633 kg (3,600 lb)	9.7	6.2
≈2,404 kg (5,300 lb)	6.2	5.5

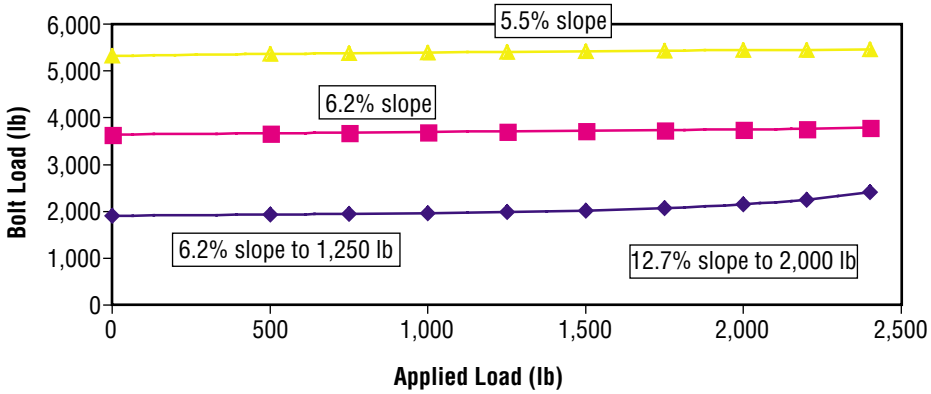

Figure 32. FEM results for change in bolt load at three preloads (long bolt).

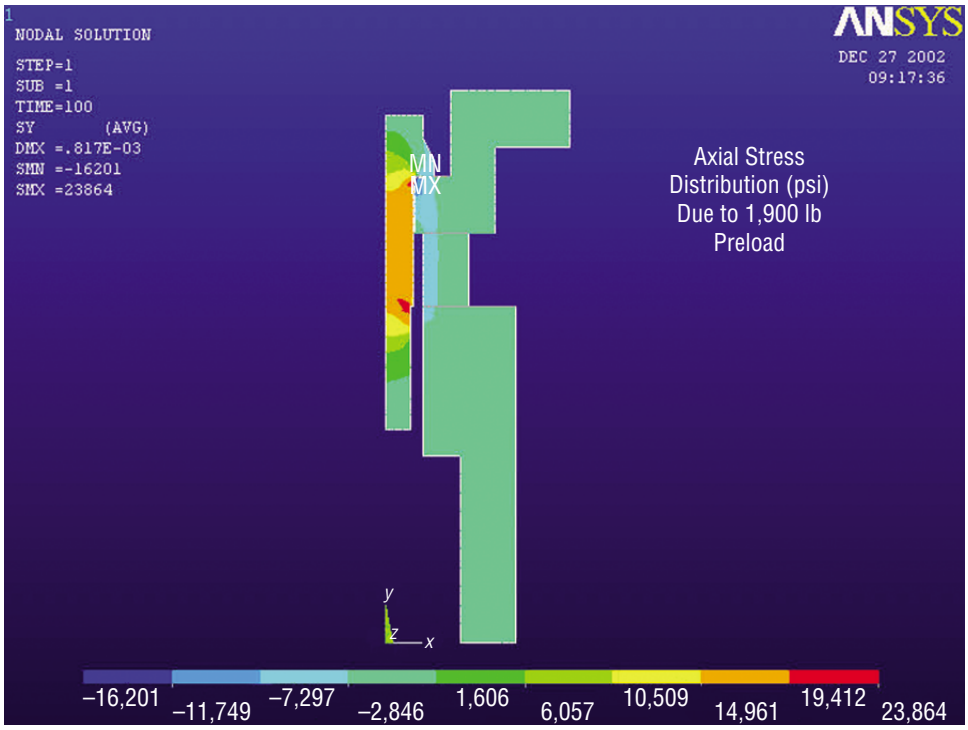

Figure 33. FEM for axial stress distribution at preload of 862 kg (1,900 lb) for long bolt.

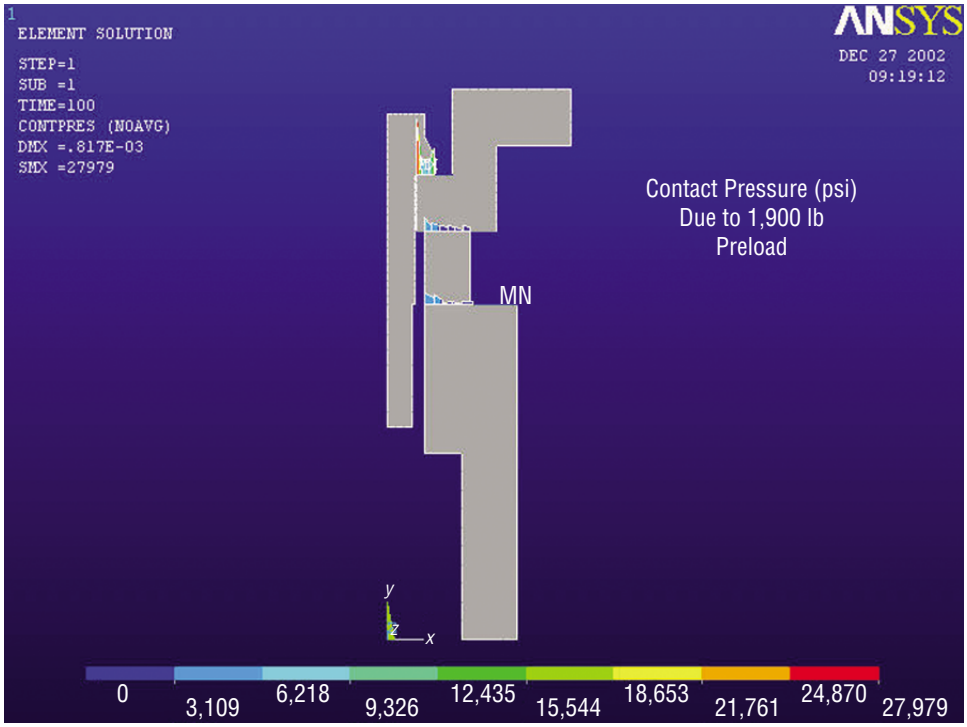

Figure 34. FEM for contact pressure distribution at preload of 862 kg (1,900 lb) for long bolt.

4.4 Other Tests and Analyses

A second set of tests was run using a Strainsert bolt of the same length as the flight bolt. These tests used the same setup and procedures discussed in section 3, with the following modifications:

- A286 stainless steel flight-length Strainsert bolt.
- No spacer.
- Insert depths taken twice—before any test began and after all tests were completed.
- Applied loads taken to a level sufficient to ensure that the connection was fully gapped.
- Four initial preload levels evaluated at 907, 1,361, 1,814, and 2,268 kg (2,000, 3,000, 4,000, and 5,000 lb).

Figure 35 summarizes these test results. Nonlinear characteristics were more pronounced for the applied load versus bolt load curves prior to overcoming preload compression effects and gapping the joint. Since the percent change in bolt load is never linear prior to gapping, it is difficult to compare these results to the classic textbook calculations, which assume that linear behavior and values of F_b can be calculated from $0.07F_e$ to $0.58F_e$ based on assumptions used for the four variables in the calculation (L_b, A_{pc}, A_{ah}, and L_{ah}).

Figures 36 and 37 show an FEM for this test configuration, which was used to analyze bolt load change versus applied load at the four preload levels. Figures 38 and 39 show typical distributions for axial stress and contact surface pressure. Figure 40 summarizes the FEM results, which are very close to the test data, as shown in the individual test versus FEM comparisons (figs. 41–44).

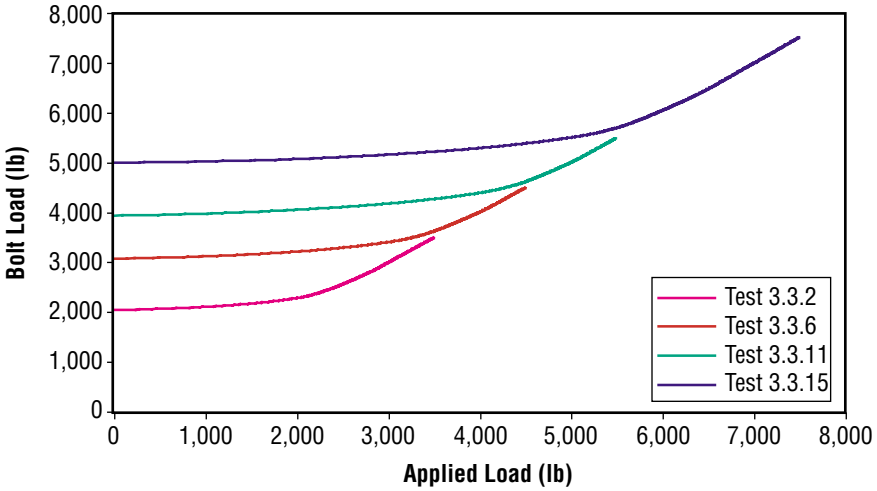

Figure 35. Step 3.3.2, 3.3.6, 3.3.11, and 3.3.15 results (flight-length bolt with insert).

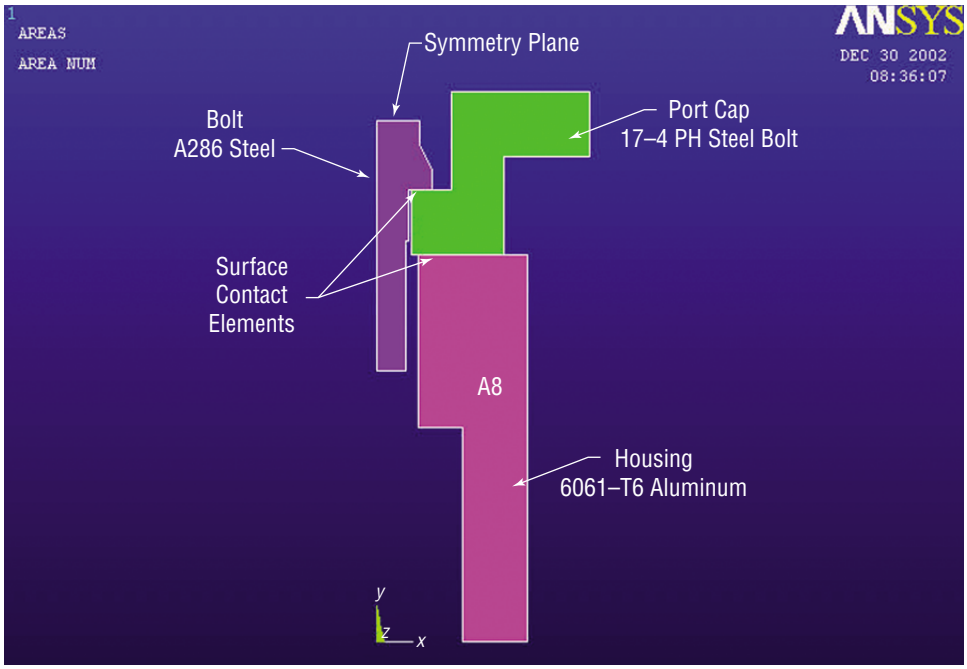

Figure 36. FEM for test configuration (flight-length bolt).

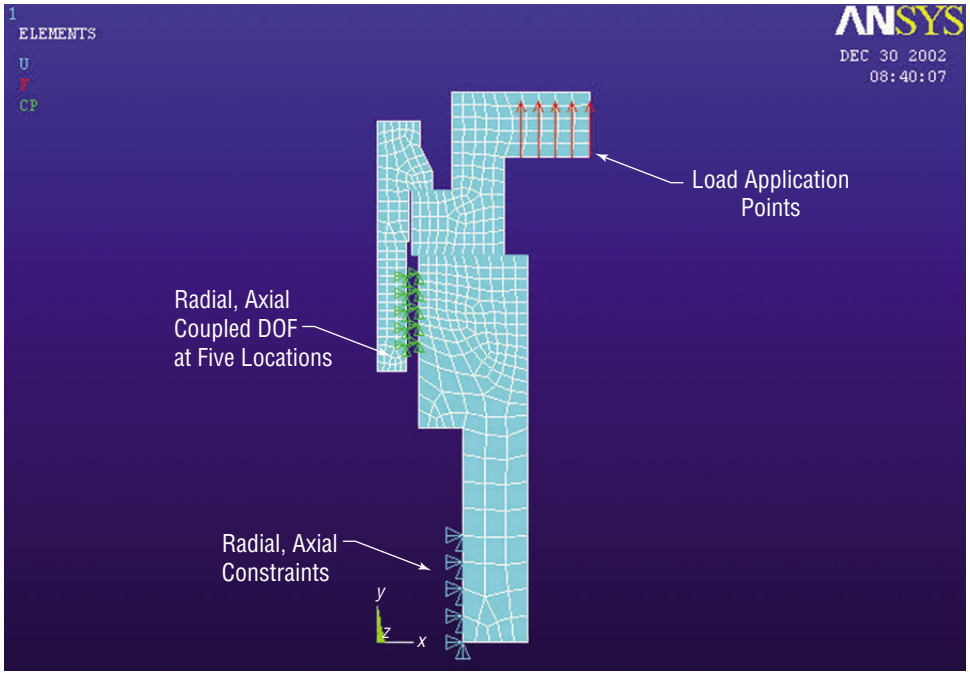

Figure 37. FEM for forces applied to test configuration (flight-length bolt).

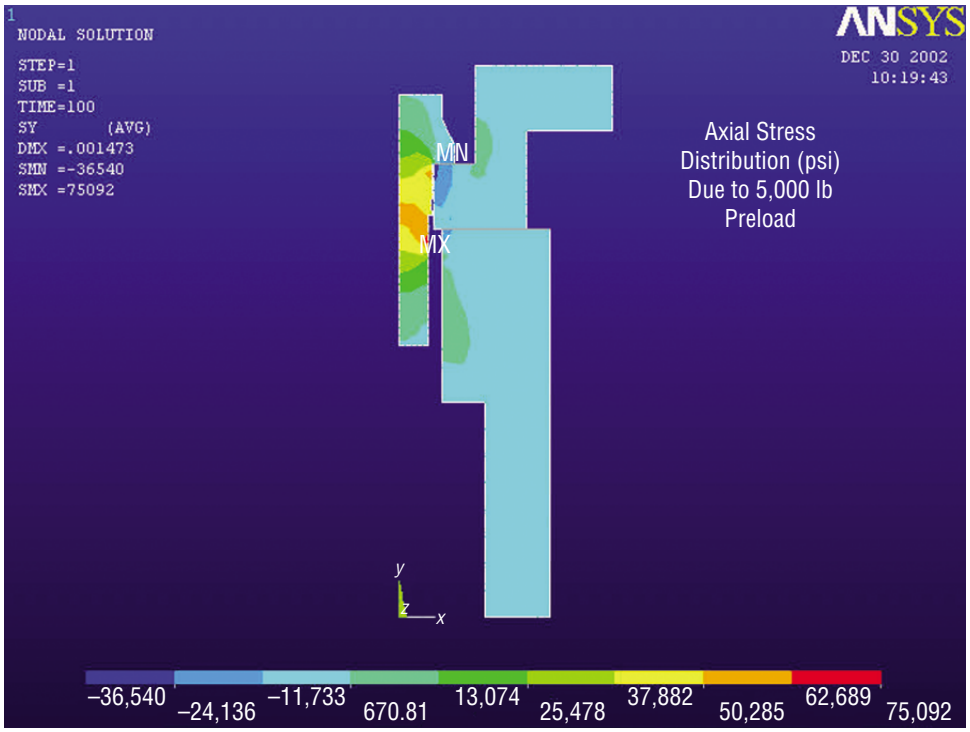

Figure 38. FEM for axial stress distribution at preload of 2,268 kg (5,000 lb) for flight-length bolt.

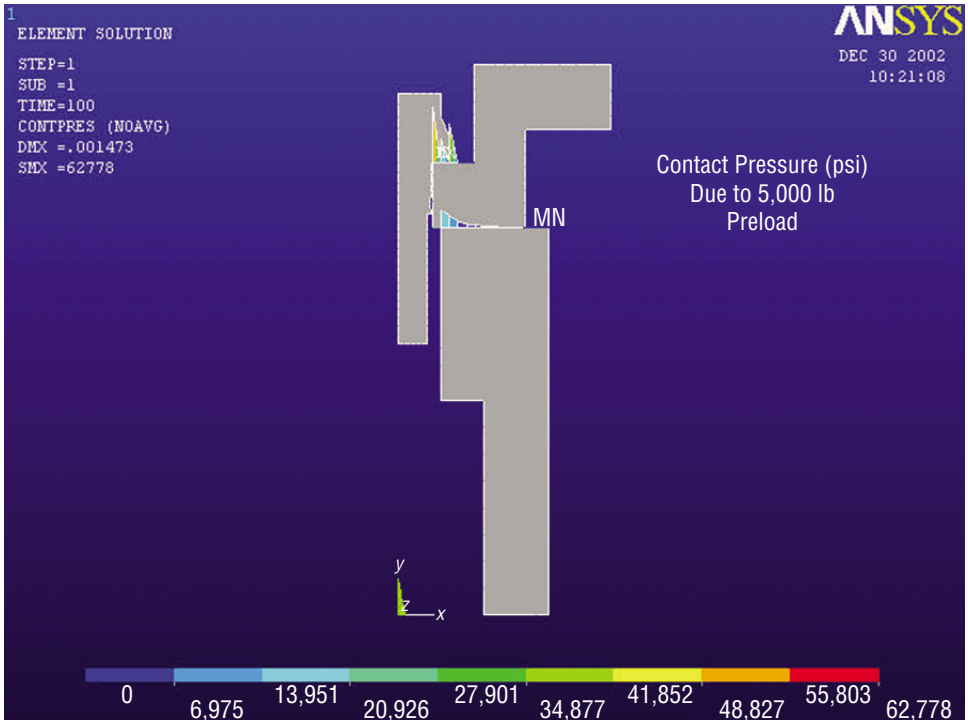

Figure 39. FEM results for contact pressure distribution at preload of 2,268 kg (5,000 lb) for flight-length bolt.

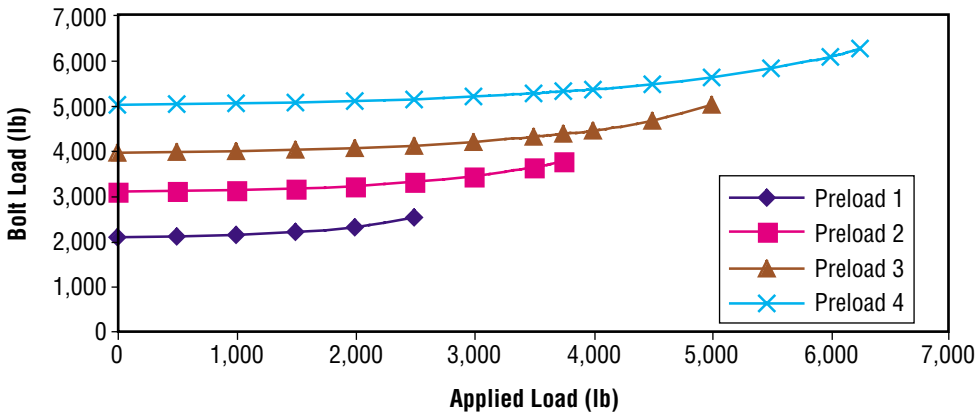

Figure 40. FEM results for change in bolt load at four preloads (flight-length bolt).

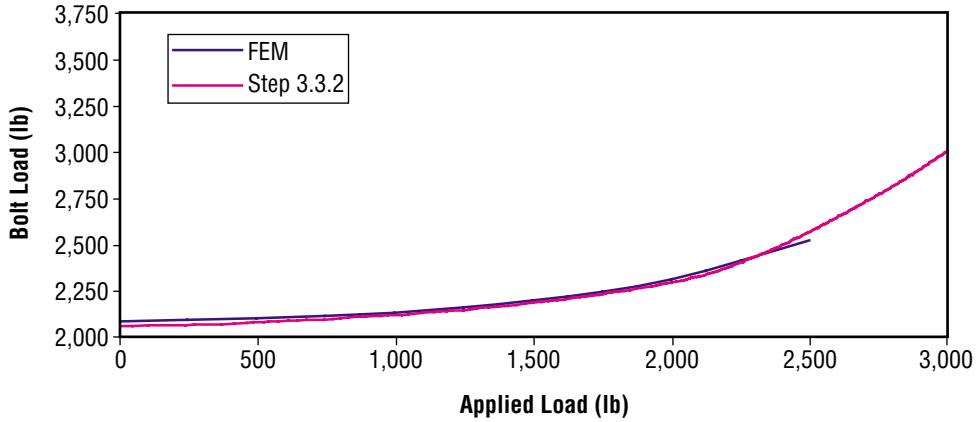

Figure 41. Step 3.3.2 versus FEM results (flight-length bolt).

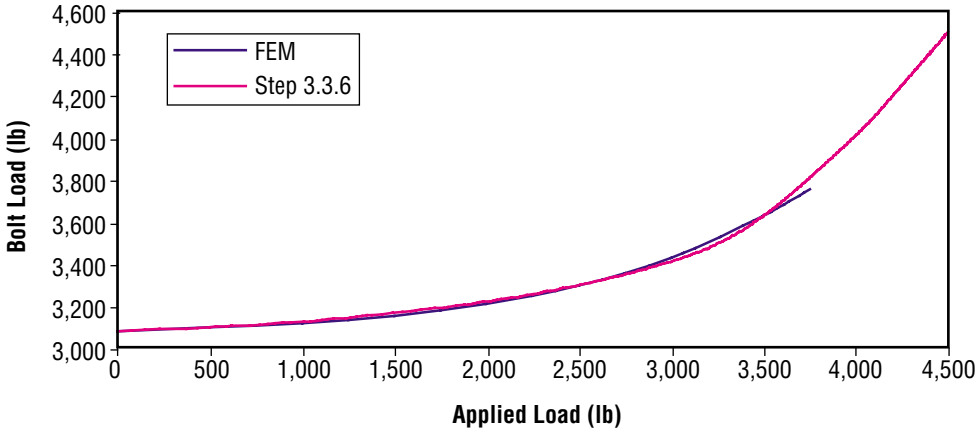

Figure 42. Step 3.3.6 versus FEM results (flight-length bolt).

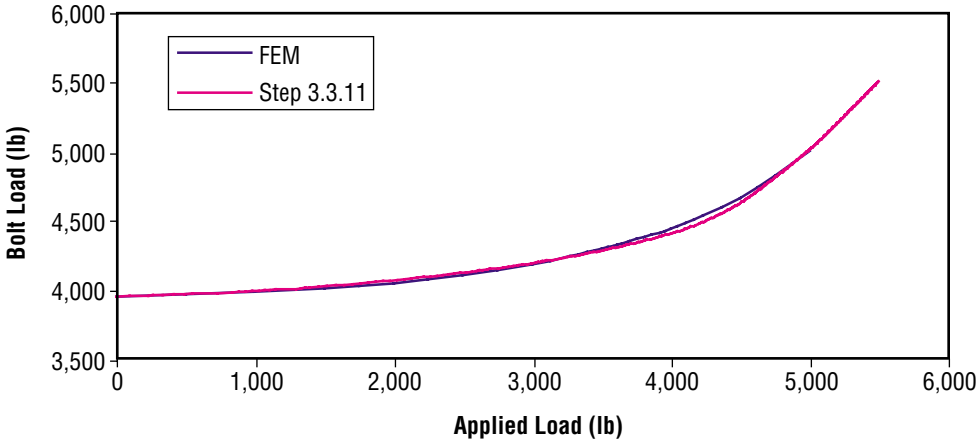

Figure 43. Step 3.3.11 versus FEM results (flight-length bolt).

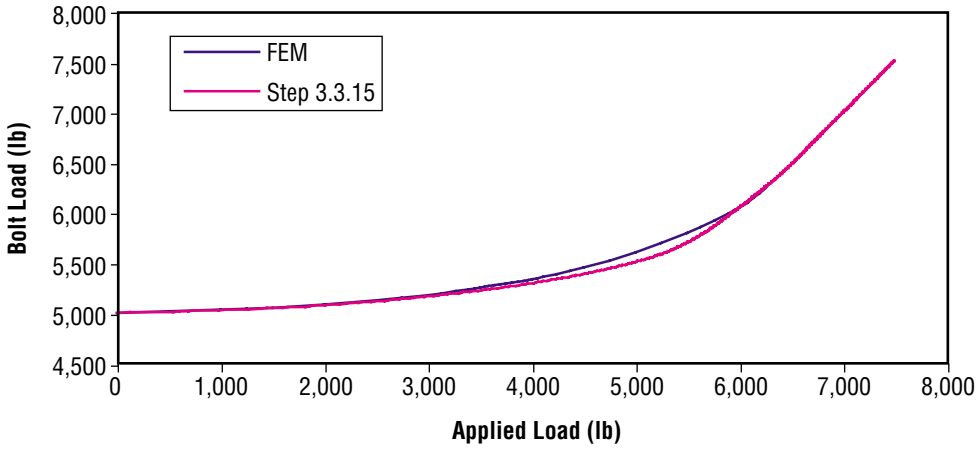

Figure 44. Step 3.3.15 versus FEM results (flight-length bolt).

5. CONCLUSIONS

The following conclusions pertain specifically to the mockup hydraulic pump port cap joint system tested:

(1) For all initial bolt preloads, bolt loads increased as the external applied loads increased.

(2) For higher initial bolt preloads, less load was transferred into the bolt, due to external applied loading.

(3) Textbook solutions can be misleading when used to determine the behavior of a preloaded joint that includes a steel bolt threaded into steel inserts in aluminum parts. However, it is possible to get good results if an FEM is carefully constructed for the connection.

REFERENCES

1. Faires, V.M.: *Design of Machine Elements*, 4th ed., pp. 164–168, Macmillan Publishing Co., New York, 1965.

REPORT DOCUMENTATION PAGE

Form Approved
OMB No. 0704-0188

1. AGENCY USE ONLY *(Leave Blank)*	2. REPORT DATE	3. REPORT TYPE AND DATES COVERED
	June 2004	Technical Memorandum

4. TITLE AND SUBTITLE
Solid Rocket Booster Hydraulic Pump Port Cap Joint Load Testing

5. FUNDING NUMBERS

6. AUTHORS
W.R. Gamwell and N.C. Murphy

7. PERFORMING ORGANIZATION NAMES(S) AND ADDRESS(ES)
George C. Marshall Space Flight Center
Marshall Space Flight Center, AL 35812

8. PERFORMING ORGANIZATION REPORT NUMBER
M–1114

9. SPONSORING/MONITORING AGENCY NAME(S) AND ADDRESS(ES)
National Aeronautics and Space Administration
Washington, DC 20546–0001

10. SPONSORING/MONITORING AGENCY REPORT NUMBER
NASA/TM—2004–213282

11. SUPPLEMENTARY NOTES
Prepared by the Materials, Processes, and Manufacturing Department, Engineering Directorate

12a. DISTRIBUTION/AVAILABILITY STATEMENT
Unclassified-Unlimited
Subject Category 26
Availability: NASA CASI (301) 621–0390

12b. DISTRIBUTION CODE

13. ABSTRACT *(Maximum 200 words)*

The solid rocket booster uses hydraulic pumps fabricated from cast C355 aluminum alloy, with 17–4 PH stainless steel pump port caps. Corrosion-resistant steel, MS51830 CA204L self-locking screw thread inserts are installed into C355 pump housings, with A286 stainless steel fasteners installed into the insert to secure the pump port cap to the housing. In the past, pump port cap fasteners were installed to a torque of 33 Nm (300 in-lb). However, the structural analyses used a significantly higher nut factor than indicated during tests conducted by Boeing Space Systems. When the torque values were reassessed using Boeing's nut factor, the fastener preload had a factor of safety of <1, with potential for overloading the joint. This paper describes how behavior was determined for a preloaded joint with a steel bolt threaded into steel inserts in aluminum parts. Finite element models were compared with test results. For all initial bolt preloads, bolt loads increased as external applied loads increased. For higher initial bolt preloads, less load was transferred into the bolt, due to external applied loading. Lower torque limits were established for pump port cap fasteners and additional limits were placed on insert axial deformation under operating conditions after seating the insert with an initial preload.

14. SUBJECT TERMS
SRB, hydraulic pump, fastener, C355 aluminum alloy, 17–4 PH stainless steel, CRES CA 204L, corrosion-resistant steel, A286 stainless steel, torque values, mechanical testing, finite element model, FEM, factor of safety, FOS

15. NUMBER OF PAGES
48

16. PRICE CODE

17. SECURITY CLASSIFICATION OF REPORT	18. SECURITY CLASSIFICATION OF THIS PAGE	19. SECURITY CLASSIFICATION OF ABSTRACT	20. LIMITATION OF ABSTRACT
Unclassified	Unclassified	Unclassified	Unlimited